Electrochemical Characterization of Co-Cr Alloys Used as Stents in Cardiovascular Applications

FLORENTINA GOLGOVICI, GEORGE RAZVAN PANDELEA DOBROVICESCU, MARIANA PRODANA*

Politehnica University of Bucharest, Faculty of Applied Chemistry and Materials Science, 1-7 Polizu Str., 011061, Bucharest, Romania

The present paper is a comparison study between some alloys based on Co and Cr metals. For the study of corrosion were used two types of alloys Co-Cr with different chemical compositions: Wirobond C and Wirobond 280 marketed by the company Bego. Methods for testing the stability of the alloys in bioliquid that simulates the electrolytes in the human body are the variation of potential in time (open circuit potential-OCP), potentiodynamic polarization tests, electrochemical impedance spectroscopy measurements (EIS) and inductively coupled plasma mass spectrometry (ICP-MS). All studied two types of alloys based on Co-Cr show a low corrosion rate in the studied environments. The presence of oxide coating decreases the release of ions in solution. The small amount of metal ions released in solution is in the domain of part per million.

Keywords: corrosion, ion release, Co-Cr alloys, ICP-MS, stability

CoCr [1, 2] and titanium alloys [3, 4] are the most investigated and used biomaterials in medical applications in the last decades with non modified and modified surface in order to improve their performance [5]. Starting with 1994 the percutaneous transluminal coronary angioplasty (PTCA) was the only treatment available for the coronary heart disease [6-8]. The incidence of coronarian restenosis is an important issue that requires repeated interventional procedures up to 30% of patients treated only with PTCA.

The coronary stents were developed to provide a metal frame for vessels requiring angioplasty to limit negative remodeling [9].

Sigwart et al. reported in 1987 early efficacy of stenting in reducing restenosis rates.

Until 1994, the Food and Drug Administration (FDA) has approved Gianturco-Roubin stent and stent Palmaz-Schatz TM. Gianturco-Roubin II stent was the first coronary stent approved by the FDA in June 1993 and consists of a flattened spiral wire attached to a longitudinal shaft made of stainless steel 316L. Palmaz-Schatz stent is a balloon expandable slotted tube made of stainless steel 316 L. General acceptance of stents occurred after publication of the BENESTENT and STRESS studies, which demonstrated the superiority stenting vs. balloon angioplasty [10].

Non-degradable stents are made of 316L stainless steel and has excellent mechanical properties and corrosion resistance. Ferromagnetism and low density leads to a non-MRI compatible stent. They are made of a material fluoroscopic faint. Examples: DESS first generation Cypher (sirolimus-eluting stent, Cordis, Warren, NJ) and Taxus (paclitaxel-eluting stent, Boston Scientific, Natick, MA).

Co-Cr stents have the following characteristics: resistance, superior radial and improving radioopacity; thin support –axes; Examples: second generation DES, XIENCE V (everolimus eluting stent, Abbott Vascular, CA) and Endeavor (zotarolimus-eluting stent, Medtronic Vascular, Santa Rosa, CA) [11-13].

Tantalum stent show excellent corrosion resistance, it can be covered with 316L SS for improving corrosion properties and biocompatibility, with high density and non-ferromagnetic properties. It is fluoroscopic visible and MRI compatible. The stent made of titanium present: excellent biocompatibility and resistance to corrosion.

Titanium based alloys can be combined with the Ni-Ti and can be coated with Ti-nitride oxide on 316 SS. Building a hierarchical periodic micro/nano-structures on nitinol and tailoring their influence on oriented endothelialization and anti-thrombosis is another new approach in enhancing thromboresistance [3]

Ni-Ti stents have the following characteristics: good biocompatibility, radial force and shape memory, it can be coated with polyurethane, titanium nitride and polycrystalline oxide to improve corrosion resistance.

The stent-IR comprising 90% platinum and 10% iridium has: excellent radiopacity and a reduction in thrombosis and endothelial inflammatory reactions. The percentage of restenosis was significantly higher (16%) than SS 316L steel stents.

Other materials used in manufacturing stents are pure Fe and Mg alloys: AE2153 and WE4357 used to make radiolucent stents. Quality criteria pertaining their use for various implants are included in the relevant legislative acts [6, 14-17].

Biodegradable stents [18] can eliminate early and late complications of plain metal stents also can restore vasoreactivity. Metallic implant should possess the following essential characteristics, but not limited to: (1) Excellent biocompatibility (non-toxic) (2) High corrosion resistance (3) Suitable mechanical properties (4) High wear resistance (5) Osseo-integration (in the case of bone prosthetics).

Our objective related to enhance metallic biomaterials for stents is to develop CoCr alloys with thromboresistance, and in this context the present paper as a first step is a comparison between stability in specific bioliquids of some alloys based on Co and Cr.

Experimental part

For the study of corrosion were used two types of alloys Co-Cr with different chemical compositions: Wirobond C (WBC) and Wirobond 280 (WBA) marketed by the company Bego.

The compositions of two alloys are given in table 1.

*email: prodana_mariana@yahoo.com; Phone: 0214023930

Table 1
CHEMICAL COMPOSITION OF THE Co-Cr ALLOYS

Alloy	Co %	Cr %	Mo %	Mn %	Si %	C %	N %	W %	Ga %	Fe %	Ce %
Wirobond C (WBC)	61	26	6	-	1	Max 0.02	-	5	-	0.5	0.5
Wirobond 280 (WBA)	60.2	25	4.8	<2	<2	-	-	6.2	2.9	-	-

Metal species used had a cylindrical shape having an area of 0.5 cm² exposed to corrosive environments. A cylindrical shape was preferred because it has a larger surface area and a small number of edges and corners that are more susceptible to corrosion.

In our experiment, we used a conventional electrochemical cell made by two electrodes: working electrode consisting essentially of one of the alloys Co-Cr (Wirobond C or Wirobond 280), the counter-electrode is the electrode of platinum (Pt) with a large area and reference electrode was used an electrode of Ag / AgCl, KCl.

The working electrode was mechanically polished, rinsed with redistilled water and ultrasonicated for 5 min in acetone to remove grease remaining impurities on the electrode surface after polishing in order to ensure a clean surface before the measurements.

There are several types of electrolyte used: saline solution (SF), SBF (simulated body fluid) or mannitol 20%.

Methods used for testing the stability of the alloys in bioliquid that simulates the electrolytes in the human body are the variation of potential in time (open circuit potential-OCP), potentiodynamic polarization tests, electrochemical impedance spectroscopy measurements (EIS) and inductively coupled plasma mass spectrometry (ICP-MS).

Open circuit potential
Electrochemical measurements [17] of the electrode open circuit potential were conducted on Co-Cr alloys passivated by electrochemical method.

It is known that the shift of electrode potential towards negative value may be associated with the cathodic reaction (acceleration of the reduction) and the displacement of potential towards positive values reflects the evolution of the anodic reaction (oxidation reaction inhibition) [18].

It can be said that the anodic displacement corresponds to the formation of a protective oxide film and shifting toward cathodic area may be associated with the reorganization of the film surface in a configuration less resistant against corrosion [19, 20].

Potentiodynamic polarization tests
Potentiodynamic polarization method have been performed with AutoLab PGSTAT 12 EcoChemie, starting from cathodic region, with very low speed of 2 mV / s to allow the corrosion process to proceed [21].

The potential of the working electrode was always measured against the saturated calomel electrode and plotted in relation to the current in the external circuit, thus obtaining anodic and cathodic polarization curves.

Electrochemical impedance spectroscopy tests
Electrochemical impedance spectroscopy procedure was made within 10^5 Hz and 10^{-1} Hz frequency range, with an *ac* voltage amplitude of 10mV; the impedances were represented as Nyquist and Bode spectra.

Mass spectrometry with inductively coupled plasma (ICP-MS)
The mass spectrometer with inductively coupled plasma has the following components: ion source (plasma to 10000K), room spray, atomizer, cones, omega lens cell reaction quadrupole mass filter and detector.

Ions are introduced into the plasma at 10000K, emits an electron resulting a positive ion. These ions are focused through the cone and the omega lenses, are separated into the mass spectrometer where it enters the magnetic resonance and the detector measure the quantity.

Ions must be separated into photons and neutral particles. With lens and octopole reaction cell, the detector (quadrupole), just get the highlights, other particles being diverted.

From the used methods were obtained significant data. From OCP method (potential variation in time) were acquired information about the stability of the oxide film formed on the surface; the corrosion resistance of alloys in simulated physiological medium fluid were obtained from potentiodynamic polarization method; electrochemical impedance spectroscopy give information about polarization resistance of alloys; by ICP-MS we measure qualitative and quantitative ions released from these alloys.

Bioliquids composition test
The simulated media were simulated physiological fluids solutions, saline solution, and mannitol: NaCl (9 g/l) and (SBF) [20]: NaCl 8.367255g; $NaHCO_3$ 5.534g; $Na_2HPO_4.2H_2O$ 22.165g; $MgCl_2.6H_2O$ 0.51359g; $CaCl_2.2H_2O$ 0.51891g; Na_2SO_4 0.071 for 1 liter of bidistilled water.

Results and discussions
The primary objective of this paper was to study the electrochemical behaviour of the two alloys based on Co-Cr in different artificial fluids, in order of their use in the manufacture of stents. The alloys chosen for the study of corrosion behavior were Wirobond 280 (WBA) and Wirobond C (WBC).

The electrochemical behavior of Co-Cr alloys in saline solution
First we studied the electrochemical behavior of the two alloys in saline solution (SF) with the following composition: NaCl (9 g / L).

Determination of open circuit potential
OCP determination was made during one hour, recording the variation of open circuit potential in time. In a first step, the potentials value of the two biomaterials shift rapidly towards electropositive values in the first minutes of immersion in the electrolyte. However, a second phase in which increase the potential (moving towards electropositive values) is slower, ending with a plateau at higher immersion time. As can be seen in figure 1, for the Co-Cr alloys studied the potential values reach stable after 1 h of immersion in saline electrolyte, the potential variation is less than 2 mV for a period of 5 min.

The trends of shifting potentials of the two studied alloys towards electropositive values suggest that the surface passive film increases continuously with increasing of immersion time. In addition, the emergence of a relatively
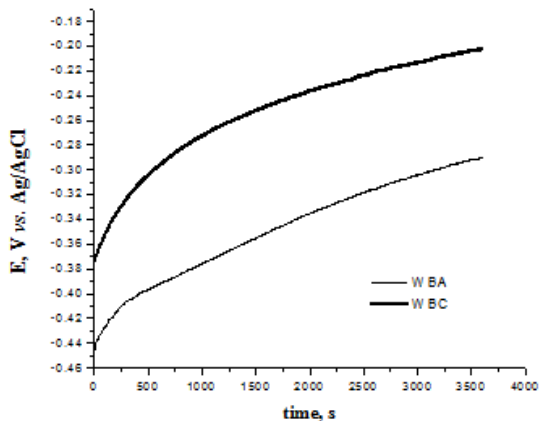
Fig.1. OCP variation in time for the two alloys in SF at 37⁰C

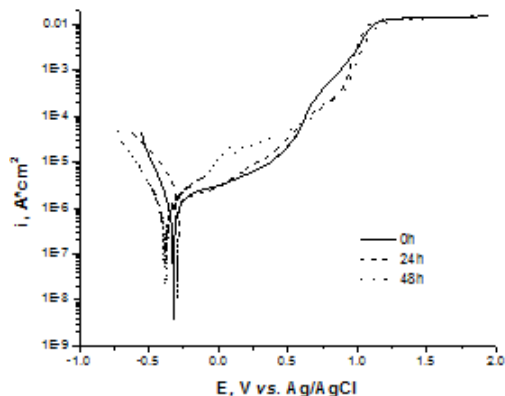Fig.3. Polarization curves of WBC alloy in SF at different immersion times

Fig. 2. Polarization curves for WBA alloy at different immersion times in SF

stable potential is an indication of a stable chemical nature of passive film.

Potentiodynamic polarization studies

To observe the behavior of two alloys in SF, polarization curves were recorded after different immersion time in the electrolyte, at 37⁰C constant temperature. First studied Co-Cr alloy was Wirobond 280 (WBA), and the curves obtained are shown in figure 2.

It can be seen that after 24 h of immersion in saline solution, is an increase in the corrosion current density, which leads to an increase of corrosion rate. After 48 h of immersion, the corrosion rate of the WBA decreases more, indicating the formation of a protective film on its surface.

In the case of the second studied alloy based on Co-Cr, Wirobond C (WBC), polarization curves recorded at different immersion times in physiological saline are shown in figure 3. It can be seen a downward trend of corrosion current density with increasing immersion time. Perhaps the alloy surface forms a protective film on which leads to slower saline corrosion of this alloy.
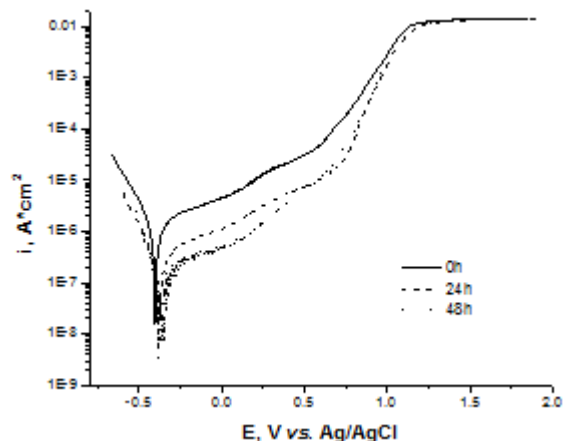
Corrosion kinetic parameters obtained from these polarization curves shown in figures 2-4 were calculated using two methods: Tafel slopes and polarization resistance method. The values obtained for the corrosion current density (i_{corr}), the corrosion potential (E_{corr}), the corrosion rate, the polarization resistance (R_p), the anodic (B_a) and cathodic Tafel slope (B_c) are shown in table 2.

The two methods yielded similar values of corrosion current density. Polarization resistance increase for WBC Co-Cr based alloy increasing immersion time in electrolyte, indicating a decrease of corrosion rate for this biomaterial in saline solution. So, as observed from polarization curves, with increase of immersion time in the corrosive solution, corrosion kinetic parameters values decrease for WBC proving that corrosion rate increase.

It can be seen that WBC has the lowest corrosion rate after 24 and 48 h of immersion.

Electrochemical impedance spectroscopy tests

Tests of electrochemical impedance spectroscopy (EIS) led to record spectra shown in the Nyquist and Bode diagrams. In figure 4 the diagrams for WBA alloy in SF at different immersion times are presented.

In figure 4a, Nyquist diagram shows the dependence of the imaginary part versus real part of impedance, whereas the Bode diagram (fig. 4b) represents simultaneously two dependences: impedance modulus versus frequency and phase angle versus frequency.

From Nyquist diagrams (fig. 4a) we can observe two capacitive semicircles, one at high frequencies and the other at low frequencies. The diameter value of the second semicircle decrease after 24 h of immersion, followed by an increase when the immersion time is 48 h. This indicates an increase of polarization resistance, which leads to a lower corrosion rate with immersion time increasing, confirming the data obtained from polarization curves.

Table 2
CORROSION KINETIC PARAMETERS FOR Co-Cr ALLOYS AT DIFFERENT IMMERSION TIMES IN SF

| Alloy	Time, h	Tafel Method						Polarization Resistance Method	
		E_{corr}, mV	i_{corr}, μA*cm⁻²	K_g, g*m⁻²h⁻¹	P, mm *year⁻¹	B_a, mV	-B_c, mV	R_p, Ω	i_{corr}, μA*cm⁻²
WBA	0	-325	0.865	0.01091	0.0112	220	300	76695	0.71859
	24	-295	1.531	0.0193	0.0199	164	280	42361	1.06013
	48	-388	0.948	0.01174	0.0121	156	108	59360	0.46683
WBC	0	-401	1.561	0.01933	0.0199	163	106	34981	0.79729
	24	-380	0.315	0.0039	0.0040	204	132	150780	0.2308
	48	-382	0.1626	0.00205	0.0021	110	180	212080	0.13979
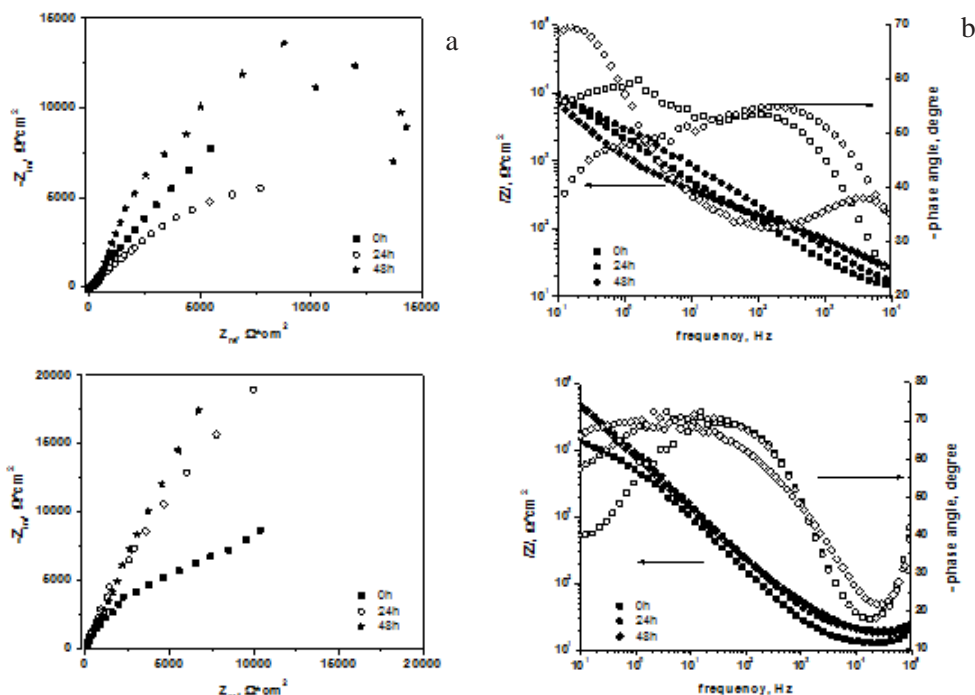
Fig. 4. Nyquist (a) and Bode (b) diagrams for WBA at different immersion time in SF

Fig. 5. Nyquist (a) and Bode (b) diagrams for WBC in SF at different immersion times

Bode diagram reveals the presence of two time constant corresponding to the two semicircles from Nyquist diagram. The second maximum phase angle value shift towards lower frequency values and increase after 48 h of immersion in SF. The value around -70° of the maximum phase angle indicates the capacitive behaviour of the interface.

The behaviour of the other Co-Cr alloy, WBC in saline solution is similar and shown in figure 5. From Nyquist diagrams (fig. 5a), we observe for WBC alloy the presence of a single open capacitive semicircle whose diameter increases with increasing immersion time in solution. This indicates an increase in polarization resistance, which leads to lower corrosion rate with immersion time increasing, thus confirming the data obtained from polarization curves. Bode diagram reveals the presence of a single time constants corresponding to one half circle in Nyquist diagram. The maximum phase angle shift towards lower frequency values and increase slightly with immersion time increasing. Maximum phase angle has values around -75° indicating the formation of a passive oxide film on the alloy surface, which leads to an almost capacitive interface response.

The electrochemical behaviour of the Co-Cr alloys in Simulated Body Fluid - SBF

Also, we studied the electrochemical behavior of the two alloys in an artificial fluid (Simulated Body Fluid - SBF).

Determination of open circuit potential

Open circuit potential in the second electrolyte studied-SBF was realized during one hour of immersion. Open circuit potential variation is shown in figure 6 for all studied Co-Cr alloys. For the two alloys, WBA and WBC we can observe a different behavior in SBF compared with SF. Open circuit potential value increased in the first 5 min, then gradually declined in the next 15 min. In the last 30 min of immersion, the potential value remained constant. It is well known that a potential shift toward negative values can be associated either with breaking and dissolving the passive film or a lack of passive film formation on alloy surface [22].
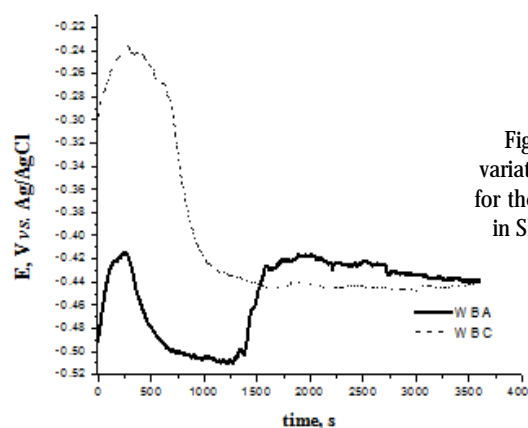

Fig. 6. OCP variation in time for the two alloys in SBF at 37⁰C

Potentiodynamic polarization study

To observe the behavior of two Co-Cr alloys in SBF, polarization curves were recorded after different immersion time in the electrolyte, at a constant temperature of 37⁰C. The curves obtained for one of the Co-Cr alloys, WBA are shown in figure 7.

As can be seen from figure 7, for WBA alloy, increasing the immersion time in SBF led to a shift of the corrosion potential towards electronegative values and a decrease of the corrosion current density value, which leads to slowing the corrosion rate. Also, it can be seen that after Tafel region, appears a passive area that move towards electropositive values and increases when immersion time increase. This phenomenon can be explained by the formation of a protective passive film on the alloy surface. For 24 and 48 h of immersion time, the value of breakdown
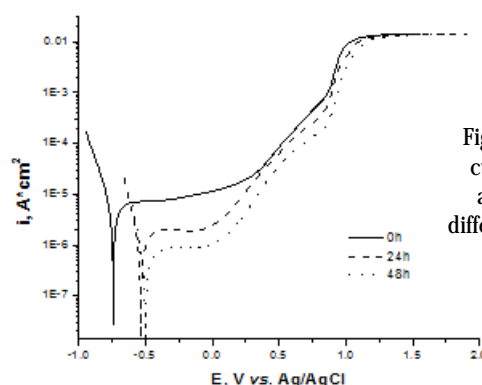

Fig.7.Polarization curves for WBA alloy in SBF at different immersion times

Table 3
KINETIC CORROSION PARAMETERS OF Co-Cr ALLOYS AT DIFFERENT IMMERSION TIMES IN SBF

| Alloy	Time, h	Tafel Method						Polarization Resistance Method	
		E_{corr}, mV	i_{corr}, $\mu A*cm^{-2}$	K_g, $g*m^{-2}h^{-1}$	P, mm $*year^{-1}$	B_a, mV	$-B_c$, mV	R_P, Ω	i_{corr}, $\mu A*cm^{-2}$
WBA	0	-714	2.87	0.03619	0.0373	197	125	15826	2.0982
	24	-533	0.725	0.00914	0.0094	204	75	81745	0.2913
	48	-498	0.309	0.0039	0.0040	210	77	155940	0.1569
WBC	0	-650	1.976	0.02447	0.0252	143	104	23901	1.0939
	24	-163	1.478	0.0183	0.0188	123	157	31822	0.9411
	48	-200	0.516	0.00639	0.0066	194	165	101920	0.3798
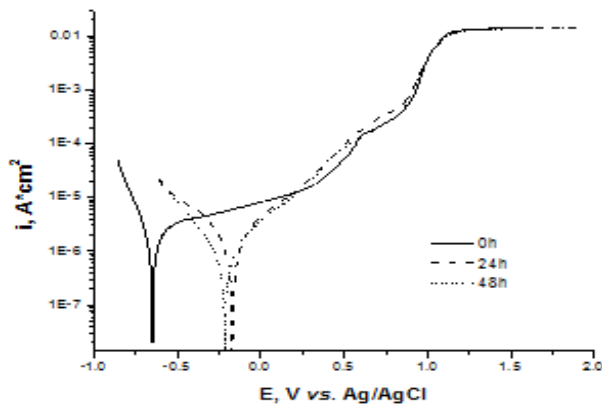
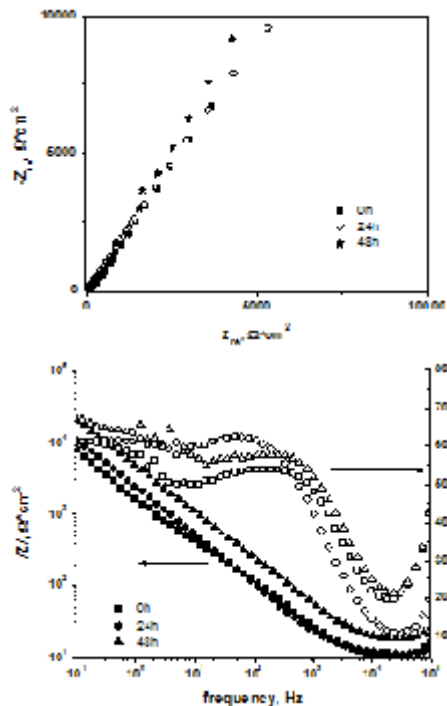Fig.8. Polarization curves for WBC alloys in SBF at different immersion times

Fig. 9. Nyquist and Bode diagrams for WBA in SBF at different immersion times

the anodic (B_a) and cathodic (B_c) slope, polarization resistance (R_p) are shown in table 3.

The two methods yielded similar values of corrosion current density. The polarization resistance increases for all studied alloys, with increasing immersion time in electrolyte, indicating a decrease in the corrosion rate of each of the biomaterials in SBF.

So as observed from the polarization curves method, increasing immersion time in the corrosive solution, corrosion kinetic parameters values decrease, proving decrease the corrosion rate of the Co-Cr alloy.

Electrochemical impedance spectroscopy test

Tests of electrochemical impedance spectroscopy (EIS) led to record spectra shown in the Nyquist and Bode diagrams. Figure 9 present the diagrams obtained for WBA after different immersion time in SBF. Bode diagrams reveal the presence of two time constants. The passive film on alloy surface is formed, leading to the establishment of two interfaces. The value of the second maximum phase angle moves towards lower values of frequency and increases with immersion time. Increasing the value from -60° to -70° for the second maximum phase angle indicates an increase in the thickness of the protective film, which leads to a decrease in the corrosion rate of the alloy in SBF. Thus confirming the data obtained by potentiodynamic polarization method.

The behaviour of the other Co-Cr based alloys in SBF is presented in figure 10. In figure 10, it can be seen that for WBC alloy two time constants appear in the Bode diagram
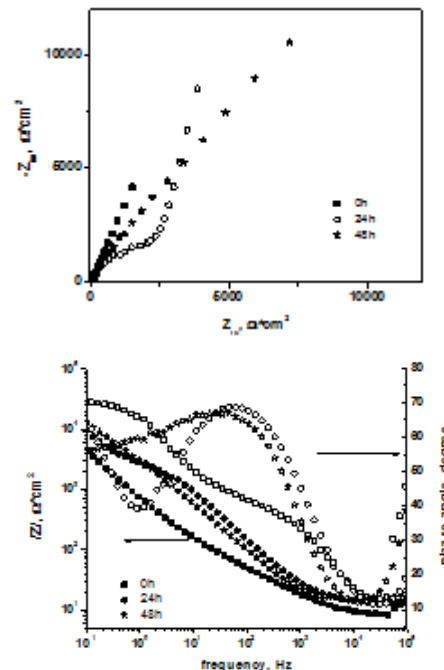

Fig. 10. Nyquist and Bode diagrams for WBC in SBF at different immersion times

potential of the passive film is around 0 V, while for the initial moment, this potential has the value around -0.4V.

For the second Co-Cr studied alloy, it was observed that increasing immersion time in SBF corrosion current density value decreases, which leads to slower corrosion (fig. 8). For these alloys, WBC, we not observed a passive region.

Corrosion kinetic parameters obtained from these polarization curves shown in figures 7, 8 were calculated using two methods: Tafel slopes extrapolation and polarization resistance. The values obtained for the corrosion potential (E_{corr}), corrosion current density (i_{corr}),

and two maximum phase angle, one at high frequencies and the other to low frequencies.

The electrochemical behaviour of the Co-Cr alloys in Mannitol

The next step was to study the electrochemical behavior of the Co-Cr based alloys in a solution with the following composition: Mannitol 20% in alcohol obtained by the reduction of mannose used as osmotic diuretic.

Open circuit potential

As in previous cases, the first step was to analyze the behavior of open circuit potential for Co-Cr alloys for one hour. In figure 11, it can be seen that there was obtained a reaction similar to that obtained in saline solution. In the first minutes after immersion occurs by sudden movement of potential to electropositive values, then the potential value remains relatively stable.
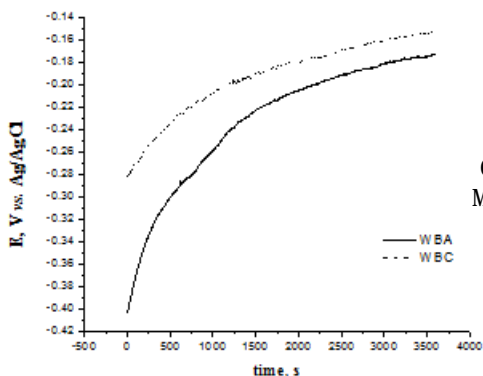
Fig. 11. OCP behaviour for Co-Cr alloys in Mannitol, at 37^{0}C

The trend of shifting potentials of the studied alloys towards electropositive values suggest that the protective passive film which covers the metal surface increase continuously with increasing immersion time in mannitol solution. In addition, the emergence of a relatively stable potential is an indication of stable chemical nature of passive film.

Potentiodynamic polarization studies

To track the behavior of Co-Cr based alloys in Mannitol, polarization curves were recorded after different immersion time in the electrolyte at 37^{0}C constant temperature. The curves obtained for one of the Co-Cr alloys, WBA, are shown in figure 12. It can be seen that with increasing immersion time in electrolyte, there is a slight shift of corrosion potential toward electropositive values. At the same time, the corrosion current density decreases, thus lowering the corrosion rate.

For WBC alloy (fig.13), after 48 h of immersion, corrosion current density increases, instead they get after Tafel region, a passive area of approximately 0.3 V.
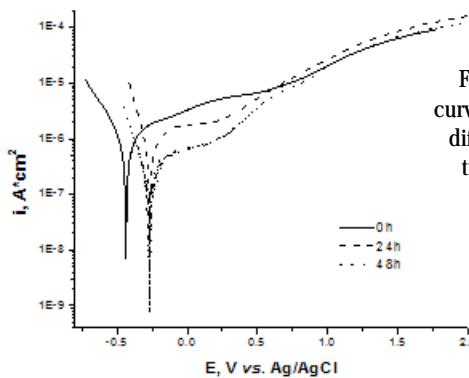
Fig.12.Polarization curves for WBA alloy at different immersion times in Mannitol
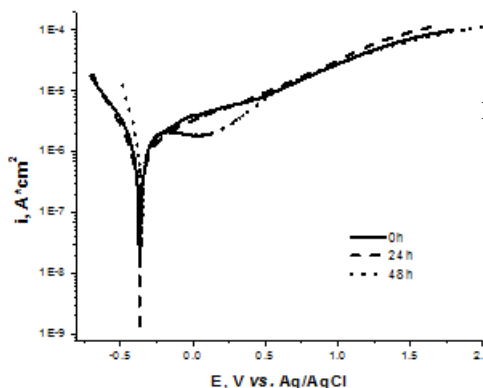
Fig.13.Polarization curves for WBC alloy at different immersion times in Mannitol

Corrosion kinetic parameters obtained from these polarization curves shown in figures 12 and 13 were calculated using two methods. The values are shown in table 4.

The two methods yielded similar values of corrosion current density. As shown polarization curves, with increasing time of immersion in the corrosive solution, corrosion kinetics parameter values grow, proving corrosion rate increase of two types of biomaterials studied.

Electrochemical impedance spectroscopy tests

Tests of electrochemical impedance spectroscopy (EIS) led to record spectra shown in the Nyquist and Bode diagrams. Figure 14 presents the diagrams obtained for WBA alloy at different immersion time in Mannitol solution. From the Nyquist diagrams we can observe that, in all cases the solution resistance is high, due to the electrolyte composition. Bode diagram reveals the presence of a single time constants corresponding to one half circle on Nyquist diagram. The maximum phase angle occurs at very low frequency and moves towards lower values with increasing immersion time in the solution. Maximum phase angle at initial moment has values around -45° indicating the emergence of a diffusion phenomenon at the alloy surface. The maximum phase angle then increases with increasing immersion time in the solution.

Table 4

KINETIC CORROSION PARAMETERS FOR Co-Cr ALLOYS AT DIFFERENT IMMERSION TIMES IN MANNITOL

| Alloy	Time, h	Tafel Method						Polarization Resistance Method	
		E_{corr}, mV	i_{corr}, $\mu A*cm^{-2}$	K_g, $g*m^{-2}h^{-1}$	P, mm $*year^{-1}$	B_a, mV	$-B_c$, mV	R_p, Ω	i_{corr}, $\mu A*cm^{-2}$
WBA	0	-421	0.464	0.00585	0.0060	146	160	94410	0.3511
	24	-260	0.385	0.00485	0.005	98	100	97180	0.2211
	48	-265	0.097	0.00122	0.0013	100	120	339470	0.0698
WBC	0	-360	0.509	0.0063	0.0065	165	150	95170	0.3585
	24	-364	0.386	0.00478	0.0049	143	162	123510	0.2670
	48	-350	0.553	0.00685	0.0070	121	97	62174	0.3760
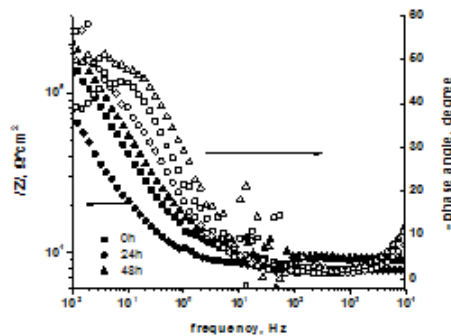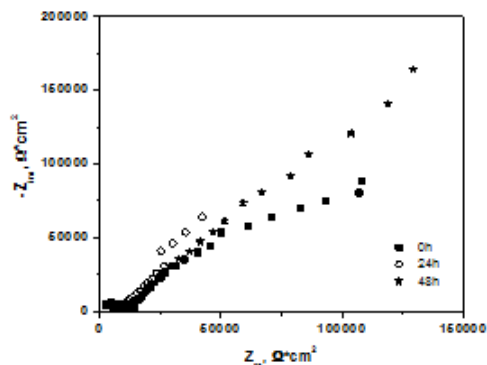
Fig. 14. Nyquist and Bode diagrams for the WBA at different immersion times in Mannitol
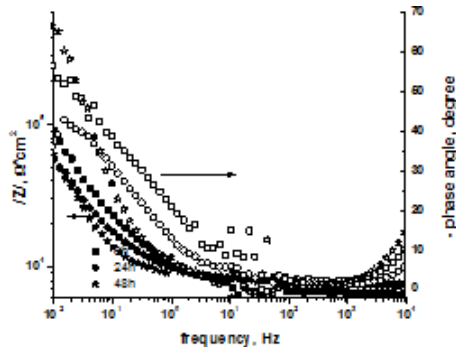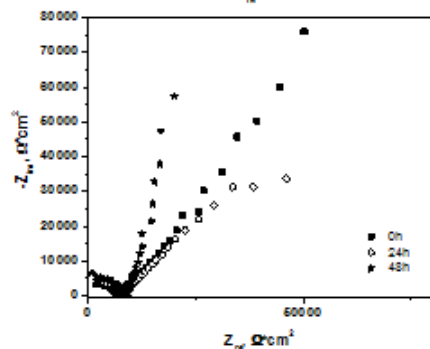

Fig. 15. Nyquist and Bode diagrams for the WBC at different immersion times in Mannitol

For WBC was obtained the same kind of behavior, Nyquist and Bode diagrams obtained are shown in figure 15.

Determination of ions released from alloys exposed to simulated physiological solutions

The concentration of metal ions released into the physiological solutions been shown using an ICP-MS, ELAN DRC-e Perkin Elmer SCIEX USA. The detection limit is 0.001μg. g^{-1}. Alloy samples [23] are immersed for different periods of time in SBF, saline NaCl 0.9% and mannitol and the solution were analyzed quantitatively. The concentration of metal ions that are released during the physiological environment simulating the conditions in the human body was obtained. It is important to know these

Table 5
OPERATING CONDITIONS FOR ICP-MS

Parameter	Value
Rf power	1500 W
Plasma gas flow	15 L min^{-1}
Aerosol gas flow	1.2 L min^{-1}
Resolution	Normal
Sweeps/reading and	5
Points/spectral peak	1
Dwell time	500 ms
Readings per replicate	400

Table 6
ICP-MS FOR SAMPLES OF ALLOYS

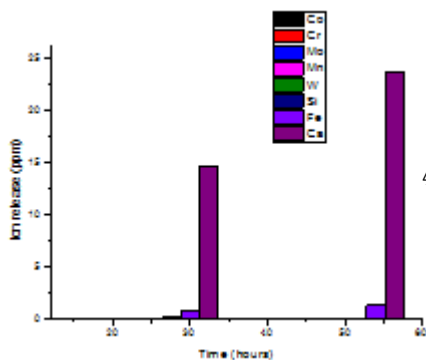| Sample	Concentration (mg/L)							
	Co	Cr	Mo	Mn	W	Si	Fe	Ca
WBC in SBF 24h	0.296	0.124	0.032	0.002	0.021	0.202	1.431	29.058
WBA in SBF 24h	0.097	0.087	0.024	0.001	0.015	0.176	0.795	14.602
WBC in SBF 48h	0.046	0.033	0.005	0.002	0.003	0.121	4.627	81.830
WBA in SBF 48h	0.086	0.029	0.012	0.001	0.006	0.144	1.327	23.769
WBC in SF 24h	0.029	0.026	0.009	0.001	0.002	0.013	0.314	4.176
WBA in SF 24h	0.042	0.053	0.016	0.001	0.005	0.014	0.293	3.941
WBC in SF 48h	0.113	0.040	0.013	0.003	0.008	0.015	0.260	2.812
WBA in SF 48h	0.048	0.013	0.008	0.002	0.002	0.014	0.249	2.887
WBC in manitol 24h	0.107	0.823	0.007	0.008	0.003	3.938	0.838	8.534
WBA in manitol 24h	0.162	0.846	0.021	0.005	0.011	4.025	0.903	6.883
WBC in manitol 48h	0.119	0.780	0.016	0.003	0.009	3.607	0.377	6.508
WBA in manitol 48h	0.112	0.788	0.011	0.012	0.006	3.767	0.364	7.369

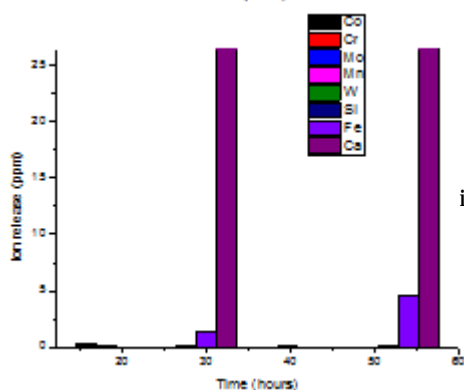Fig. 16. WBA ion release after 24 and 48 h of immersion in SBF

Fig. 17. WBC ion release after 24 and 48 h of immersion in SBF

concentrations because it is known that small amounts of metal ions can cause severe poisoning.

Liquid samples are introduced by means of the suction system in a nebulizer that generates vapor in situ at high temperature plasma. The reagents used in the calibration curves are reactive Merck. They are also used diluents comprising 1000 mg . L^{-1} in 1% v / v HNO_3 to obtain five different dilutions of 10, 50, 100, 200, 300 ppb, to trace the specific calibration curve of each element in the alloy.

As we can observe in figures 17 and 18, the ions are released into the SBF at a lower level for WBA after 24 h of immersion than for WBC.

Conclusions

All studied Co-Cr based alloys show a low corrosion rate in the studied environments. The trend of shifting potentials of the studied alloys in SF towards electropositive values suggest that on the metal surface is a protective passive film that continuously increases with increasing immersion time. Increasing the immersion time led to lower corrosion current density, decreasing the corrosion rate in almost all cases studied. In SF after an immersion time of 24 h, the lowest corrosion rate has WBC. After 48 h of immersion, the best behavior has WBC. For WBC immersed in SBF solution the potential shift towards electronegative values, which can be associated either with breaking and dissolving the passive film or with the lack of formation of passive film on the surface of the alloy. In SBF, WBA has good resistance to corrosion. Electrochemical impedance spectroscopy tests confirmed the results of the potentiodynamic polarization method. The Nyquist diagrams reveals two capacitive semicircles one at high frequencies and the other at low frequencies. Bode diagram reveals the presence of two time constant corresponding

to the two semicircles in Nyquist diagram. The formation of oxide layer has a positive effect on corrosion resistance of the metal substrate and decreases the corrosion current density being a clear advantage of preventing the release of ions in physiological solution. The presence of oxide coating lowers the amount of ions in solution. The small amount of metal ions released is ppm. Further studies are required in order to improve functional properties of vascular stents.

References

1. GOLGOVICI F., PRODANA M., POPESCU A., Rev Chim, (Bucharest) **66**, 2015, p 660
2. IONITA D., MAN I., DEMETRESCU I., Key Eng. Mater,. **330-332**, 2007, p 545
3. NOZAKI K., SHINONAGA, T.EBE, HORIUCHI N., NAKAMURA N., ,TSUTSUMI M., HANAWA Y., TSUKAMOTO M., YAMASHITA K., NAGAI A, Mat Sci Eng C, **57**, 2015, Article number 5599
4. MAN I., PIRVU C., DEMETRESCU I., Rev. Chim. (Bucharest), **59**, no. 6, 2008, p 615
5. IONITA D., UNGUREANU C., DEMETRESCU I., J Mater Eng Perform, **22**, 2013, p 3584
6. PASZENDA Z., Forming of physicochemical properties of coronary stents made of Cr-Ni-Mo steel applied in interventional cardiology. Printing House of the Silesian University of Technology, Gliwice 2005
7. PENG T., GIBULA P., YAO K., GOOSEN M., Biomaterials, **17**, 1996, p. 685
8. I. VERWEIRE, E. SCHACHT, B. QIANG, K. WANG, J MATER SCI-MATER M, **11**, 2000, p. 207
9. PASZENDA Z., J. Achiev. Mater. Manuf. Eng., **43**, no.1, 2010, p. 125
[10]. SERRUYS P., KUTRYK M. M., Handbook of coronary stens. Martin Dunitz Ltd. 1998.
11. COLOMBO A., STANKOVIC G., MOSES J., J Am Coll Cardiol, **6**, 2002, p. 1021
12. MARCINIAK J., PASZENDA Z., WALKE W., TYRLIK-HELD J., KAJZER W., Stents in minimally invasive surgery, Printing House of the Silesian University of Technology, Gliwice 2006 (in Polish).
13. SERRUYS P., RENSING B., Handbook of coronary stents. Martin Dunitz Ltd. 2002.
14. *** ISO 5832/1:2007 Implants of surgery - metallic materials - Part 1: Wrought stainless steel.
15.*** EN 12006/3:1998 Non-active surgical implants - Part 3: Intravascular devices.
16.*** EN ISO 14630:1997 Non-active surgical implants - General requirements.
17. PRODANA M., CAPOSI M., IORDACHESCU D., IFMBE Proceedings-14th Nordic-Baltic Conference on Biomedical Engineering and Medical Physics, **20**, 2008, p. 60
18. MARECI D., BOLAT G., IZQUIERDO J., CRIMU C., MUNTEANU C., ANTONIAC I., SOUTO R.M. , Mat Sci Eng C, **60**, 2016, p 402
19. ADAMSON, A.W.A.G., A.P., Physical Chemistry of Surfaces. 6th ed., John Wiley and Sons, 1997.
20. MENINI R., DION M.J., SO S.K.V., GAUTHIER M., LEFEVRE L.P., J. Electrochem. Soc., **153**, no. 1, 2006, p. B13
21.GOLGOVICI F., PRODANA M., IONIÃ D., Metode avansate de caracterizare a biomaterialelor, Ed.Printech, Bucure'ti, 2011.
22. SHI D., Biomaterials and Tissue Engineering. Spirnger-Verlag Berlin Heidelberg, Germany 2004.
23. APS J.K.M., MARTENS L.C., Forensic Sci Int, **150**, 2005, p. 119